

# Experimental and numerical study on acceleration of flyer plate by overdriven detonation of insensitive high explosive

Xiangli Guo<sup>\*</sup>, Yong Han<sup>\*</sup>, Wei Cao<sup>\*,\*\*\*†</sup>, Zhenyu Zhang<sup>\*\*</sup>, Luchuan Jia<sup>\*</sup>, and Hui Ye<sup>\*</sup>

<sup>\*</sup>Institute of Chemical Materials, China Academy of Engineering Physics, Mianyang, Sichuan 621999, CHINA

Phone: +86-816-2485366

<sup>†</sup>Corresponding author: weicao@caep.cn

<sup>\*\*</sup>College of Science, National University of Defense Technology, Changsha, Hunan 410073, CHINA

<sup>\*\*\*</sup>Department of Mechanical Engineering, McGill University, Montreal, Quebec H3A 0C3, CANADA

Received: May 8, 2017 Accepted: October 11, 2017

## Abstract

This paper presents an experimental and numerical study on the acceleration of flyer plate by the application of overdriven detonation of insensitive high explosive (IHE). The acceleration system is the multi-stage launcher system, which is also called as planar acceleration system. Two cases of different impact velocities are used in the experiment. The velocity histories of the impactor and flyer plate are measured by the velocity interferometer system for any reflector (VISAR). In order to simulate the overdriven detonation of IHE, the modified model proposed by ourselves is used. Through numerical study, the computed velocity histories of the impactor and flyer plate agree well with the experimental data. Moreover, the calculated pressure histories in the sample explosive show a steady overdriven detonation for a higher impact velocity while a Chapman-Jouguet (CJ) detonation to overdriven detonation transition for a lower impact velocity.

**Keywords:** overdriven detonation, high insensitive explosive, flyer plate ; acceleration, numerical study

## 1. Introduction

Overdriven (supracompressed) detonation is a detonation process that can provide a higher or much higher detonation pressure and propagating velocity than does the Chapman-Jouguet (CJ) detonation. Making use of the detonation products from the overdriven detonation to push the plate may lead to a hypervelocity status unachievable by means of the usual explosive acceleration techniques.

Overdriven detonation of solid explosives can be achieved by impacting them on flyer plates at velocities of several kilometers per second, and by driving with a more powerful explosive<sup>1</sup>. The flyer plates can be accelerated by light-gas gun<sup>2-4</sup>, or by explosive techniques<sup>5,6</sup>. One of the explosive techniques is the multi-stage launch system using explosive as the driving sources, which has the resembling planar geometrical arrangement used by

respective workers<sup>7,8</sup>. In the recent more than ten years, the numerical study of the explosively driven flyer plates has been widely conducted. Liu *et al.*<sup>9</sup> studied the hypervelocity acceleration of flyer plates by overdriven detonation of PETN (pentaerythritol tetranitrate)-based explosive, using the Jones-Wilkins-Lee (JWL)<sup>10</sup> equation of state (EOS). Lian *et al.*<sup>11</sup> also simulated the explosively driven metal using JWL EOS by material point method.

Practically, the flyer impact initiation of explosive is achieved by a microscopic hot spots generation and subsequent chemical reaction growth from those hot spots which may cause shock-to-detonation transition (SDT). The reaction rate models which describe SDT in explosives have been developed in recent decades. Such as the Forest Fire model<sup>12</sup>, the Ignition and Growth model<sup>13</sup>, Tang's (Johnson-Tang-Forest, JTF) model<sup>14</sup> and Kim's model<sup>15</sup>. After that, Zhang *et al.*<sup>16</sup> proposed a

modified model based on Kim's model which is more suitable to overdriven detonation.

However, the overdriven detonation phenomenon of insensitive high explosive (IHE) has not been intensively studied<sup>17)</sup>. The main purposes of this paper are to measure and hydrodynamically model the reaction zones of overdriven detonation waves in solid IHE containing TATB (1,3,5-triamino-2,4,6-trinitrobenzene). The modified model proposed by Zhang et al.<sup>16)</sup> was used in the numerical study.

## 2. Experimental setup

The planar acceleration system is illustrated in Figure 1. A planar wave generator was initiated by an instant detonator and a cylindrical pressed booster (TNT,  $1.60 \text{ g} \cdot \text{cm}^{-3}$ ,  $\phi 20 \text{ mm} \times 20 \text{ mm}$ ), then a planar shock wave initiated the cylindrical pressed loading explosive charge (explosive I, 95 wt % HMX / 5 wt % binder,  $1.86 \text{ g} \cdot \text{cm}^{-3}$ ,  $\phi 100 \text{ mm} \times 20 \text{ mm}$ ). The detonation products from the loading explosive accelerated the impactor (copper,  $\phi 70 \text{ mm} \times 1 \text{ mm}$ ) to a speed which is higher than the CJ particle velocity. The impactor impacted and initiated the cylindrical pressed sample explosive charge (explosive II, 95wt% TATB/5wt% binder,  $1.888 \text{ g} \cdot \text{cm}^{-3}$ ,  $\phi 50 \text{ mm} \times 5 \text{ mm}$ ), then the sample explosive drove the flyer plate (copper,  $\phi 40 \text{ mm} \times 2 \text{ mm}$ ). All the explosives were manufactured and provided by Institute of Chemical Materials, China Academy of Engineering Physics. The CJ properties of explosives I and II are listed in Table 1. The velocity interferometer system for any reflector (VISAR)<sup>18)</sup> was used to measure the velocity histories of impactor and flyer. VISAR measures the velocity history of a moving surface by measuring the velocity dependent phase change of laser light reflected from the surface. Two fiber probes aimed at the symmetric points 30 mm away from the center of the impactor to measure the velocity histories individually. Meanwhile, another fiber probe aimed at the center part of flyer on the back free surface to measure the velocity history of the flyer.

In this research, we chose two different impacting velocities of  $\sim 2800 \text{ m} \cdot \text{s}^{-1}$  and  $\sim 3500 \text{ m} \cdot \text{s}^{-1}$  by adjusting  $l_1$  (the spacer between explosive I and impactor) and  $l_2$  (the spacer between impactor and explosive II). Meanwhile, since the overdriven detonation is an unsteady process and is easily affected by the rarefaction wave coming from the backward detonation products to be converted into the common CJ detonation, explosive II should be arranged with a shorter length to overcome such influence<sup>9)</sup>.

## 3. Numerical methodology

In this paper, the numerical simulation was carried out in two separate steps since it is difficult for us now to accomplish the whole calculation at one time. First we calculated the flying speed of the impactor under the loading of explosive I. Secondly we calculated the acceleration process of the flyer plate from the action of explosive II. It must be noted that the second step was the focus of this system.

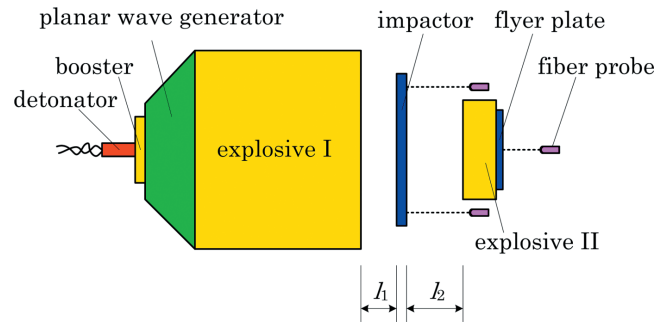


Figure 1 Schematic of the planar acceleration system.

Table 1 Champan-Jouguet properties of explosives I and II.

| Explosives | Pressure $p_{CJ}$ [GPa] | Detonation velocity $D_{CJ}$ [ $\text{km} \cdot \text{s}^{-1}$ ] |
|------------|-------------------------|--|
| I          | 36.8                    | 8.862  |
| II         | 27.7                    | 7.655  |

The numerical simulation of the velocity was simulated by the explicit finite element program ANSYS LS-DYNA. The copper metal was modeled to be an elastic-perfectly-plastic material with the von Mises yield criterion for the distinction of elastic and plastic deformation regimes. The hydrodynamic component (hydrostatic pressure) of the stresses was calculated from Mie-Grüneisen form of the equation of state (EOS) using a linear Hugoniot relationship, which is established from the experimental relation of shock velocity and particle velocity,  $U_s = C + SU_p$ , as standard reference<sup>19)</sup>. The expression of Mie-Grüneisen EOS is then given as:

$$p = \frac{C^2(V_0 - V)}{[V_0 - S(V_0 - V)]^2} \left( 1 - \frac{\Gamma}{2} + \frac{\Gamma V}{2V_0} \right) + \frac{\Gamma E}{V_0} \quad (1)$$

where  $p$  is the pressure,  $C$  is the sound speed of the material,  $S$  is the slope of the  $U_s - U_p$  curve,  $V_0$  is the initial relative volume,  $V$  is the relative volume,  $\Gamma$  is the Grüneisen coefficient, and  $E$  is the internal energy.

The JWL EOS of the reaction products of the CJ detonation was used for the assumed instantaneous detonation of explosive I. The planar wave generator was simplified as linear initiation and a certain mass of explosive I<sup>20)</sup>. The JWL parameters of explosive I are listed in Table 2.

In the simulation of the velocity of flyer plate, we used the principle proposed by Kim<sup>15)</sup> to build a pore collapse model for hot-spot ignition in shocked multi-component explosives. In the simplified numerical model, we only considered impactor impacting on and initiating explosive II and explosive II driving flyer plate. The impactor was assumed to move at a prescribed velocity determined on the basis of the experimental result and also to keep an undeformed shape before its impact onto explosive II. A reactive hydrodynamic model used for the explosive consists of two JWL EOS (one for the unreacted explosive and one for its reaction products) and one reaction rate equation. The JWL EOS is described as follows:

**Table 2** Model parameters for copper, explosive I and II.

| 1. Grüneisen parameters of copper ( $\rho_0 = 8.90 \text{ g}\cdot\text{cm}^{-3}$ )   |  |  |
|--|--|--|
| $C = 0.3958 \text{ cm}\cdot\mu\text{s}$ ; $S = 1.497$ ; $\Gamma = 2.0$ ; $V_0 = 1$   |  |  |
| 2. JWL parameters of the CJ detonation for explosive I ( $\rho_0 = 1.86 \text{ g}\cdot\text{cm}^{-3}$ )  |  |  |
| $D = 0.8835 \text{ cm}\cdot\mu\text{s}^{-1}$ ; $P_{CJ} = 36.8 \text{ GPa}$ ; $A = 852.4 \text{ GPa}$ ; $B = 18.02 \text{ GPa}$ ; $R_1 = 4.55$ ; $R_2 = 1.3$ ; $\omega = 0.38$ ; $E_0 = 10.2 \text{ GPa}$ |  |  |
| 3. Hot-spot ignition parameters for explosive II ( $\rho_0 = 1.888 \text{ g}\cdot\text{cm}^{-3}$ )   |  |  |
| Unreacted JWL  | Product JWL  | Reaction rate model  |
| $A = 77810 \text{ GPa}$  | $A = 531.396 \text{ GPa}$                                | $Z = 3.18\text{E} \times 10^{19} \mu\text{s}^{-1}$                             |
| $B = -5.031 \text{ GPa}$   | $B = 2.70309 \text{ GPa}$                                | $T^* = 30140.8 \text{ K}$  |
| $R_1 = 11.3$   | $R_1 = 4.1$  | $T_0 = 298 \text{ K}$  |
| $R_2 = 1.13$   | $R_2 = 1.1$  | $C_p = 1.4 \times 10^{-5} \text{ cm}^2\cdot\mu\text{s}^{-2}\cdot\text{K}^{-1}$ |
| $\omega = 0.8938$  | $\omega = 0.46$  | $k = 8 \times 10^{-5} \text{ Mbar}$  |
| $C_V = 2.487 \times 10^{-3} \text{ GPa}\cdot\text{K}^{-1}$   | $C_V = 1.0 \times 10^{-3} \text{ GPa}\cdot\text{K}^{-1}$ | $Q = 2.510 \times 10^{-2} \text{ cm}^2\cdot\mu\text{s}^2$                      |
| $T_0 = 298 \text{ K}$  | $E_0 = 6.9 \text{ GPa}$                                  | $k^* = 8.0 \times 10^{-14} \text{ cm}\cdot\mu\text{s}^{-1}\cdot\text{K}^{-1}$  |
| shear modulus=4.54 GPa   |  | $r_i = 0.0039 \text{ cm}$  |
| yield strength=0.2 GPa   |  | $r_o = 0.01 \text{ cm}$  |
|  |  | $a = 2.519 \times 10^{-2}$   |
|  |  | $n = 1.985$  |
|  |  | $G = 400$  |
|  |  | $z = 2.9$  |
|  |  | $m = 1.0$  |

$$p = A \exp(-R_1 V) + B \exp(R_2 V) + \frac{\omega C_V T}{V} \quad (2)$$

where  $p$  is the pressure in megabars,  $V$  is relative volume,  $T$  is the temperature,  $\omega$  is the usual Grüneisen coefficient,  $C_V$  is the average heat capacity at constant volume, and  $A$ ,  $B$ ,  $R_1$ , and  $R_2$  are constants. The reaction rate is described as follows:

$$\frac{d\lambda}{dt} = \frac{d\lambda_h}{dt} + \frac{3\lambda^{2/3}}{r_o} a p^n + G p^z (1 - \lambda)^m \quad (3)$$

where  $\lambda$  is the overall reaction rate,  $t$  is time,  $\lambda_h$  is the reaction rate of hot spot ignition,  $r_o$  is the outer radius of the hollow sphere model<sup>15)</sup>, and  $a$ ,  $n$ ,  $G$ ,  $z$ , and  $m$  are constants related to material properties. This three-term reaction rate law represents the three stages of reaction generally observed during shock initiation and detonation of pressed solid explosives. The first stage of reaction is the formation and ignition of hot spots caused by the various possible mechanisms discussed for impact ignition as the initial shock or compression wave interacts with the unreacted explosive molecules. The first term in Equation (3) is original from Kim<sup>15)</sup>, this model describes the hot spot behavior, with a help of minimum amount of experimental data, explaining the effects of properties of the component explosive material, initial particle size, initial porosity, initial binder volume fraction, initial temperature, and the applied stress. The reaction rate of hot spot ignition is obtained as follows:

$$\frac{d\lambda_h(x, t)}{dt} = \int_{r_i}^{r_o} \frac{\frac{d\Lambda}{dt}(r, x, t) 4\pi r^2}{\frac{4}{3}\pi(r_o^3 - r_i^3)} dr \quad (4)$$

$$\frac{d\Lambda}{dt} = (1 - \Lambda) Z \exp\left(-\frac{T^*}{T(r, x, t)}\right) \quad (5)$$

$$T = T_0(r, x, t) + \int_0^t \frac{dT}{dt}(r, x, t) dt \quad (6)$$

$$\frac{dT}{dt} = \frac{2.25\gamma(p_o - p_g - 2\sqrt{3}k \ln(r_o/r_i))^2}{\rho C_p (r_i^{-3} - r_o^{-3})^2 r^6} + \frac{1}{\rho C_p r^2} \frac{\partial}{\partial r} \left( r^2 k^* \frac{\partial T}{\partial r} \right) + \frac{Q}{\rho C_p} \frac{d\Lambda}{dt} \quad (7)$$

where  $r$  is the space coordinate in a hollow sphere model,  $x$  is the macro coordinate in explosive,  $r_i$  is the inner radius of the hollow sphere (*i.e.* the radius of pore),  $\Lambda(r, x, t)$  is the local degree of reaction,  $k$  is shear yield strength,  $Z$  is the pre-exponential factor in Arrhenius kinetics,  $T^*$  is the activation temperature,  $T_0$  is the initial temperature,  $p_o$  is the applied pressure,  $p_g$  is the gas pressure in the pore,  $\rho$  is the density,  $k^*$  is the thermal conductivity,  $C_p$  is the heat capacity at constant pressure,  $Q$  is the reaction heat of the explosive, and  $\gamma$  is the constants related to the viscosity of explosive. The second term in Equation (3) describes the relatively low reaction rate at the early stage of chemical reaction just after hot spots are created (low pressure), which is also proposed by Kim<sup>15)</sup>. The third term in Equation (3) describes the relatively high reaction rate at a higher pressure, which is proposed by Zhang *et al.*<sup>16)</sup>. These parameters can be determined by the thermodynamic parameters of the explosive. All the values of hot-spot ignition parameters for explosive II are also presented in Table 2.

#### 4. Results and discussion

We can get the velocity of the impactor from the

**Table 3** Results of the two impacting cases.

| Case no. | $l_1$<br>[mm] | $l_2$<br>[mm] | Impact velocity [ $\text{m}\cdot\text{s}^{-1}$ ] |           | Final velocity of flyer plate [ $\text{m}\cdot\text{s}^{-1}$ ] |           |
|----------|---------------|---------------|--|-----------|--|-----------|
|          |               |               | Experimental                                     | Numerical | Experimental   | Numerical |
| 1        | 0             | 19.70         | 3445   | 3425      | 2795   | 2754      |
| 2        | 19.95         | 11.75         | 2801   | 2808      | 1960   | 1947      |

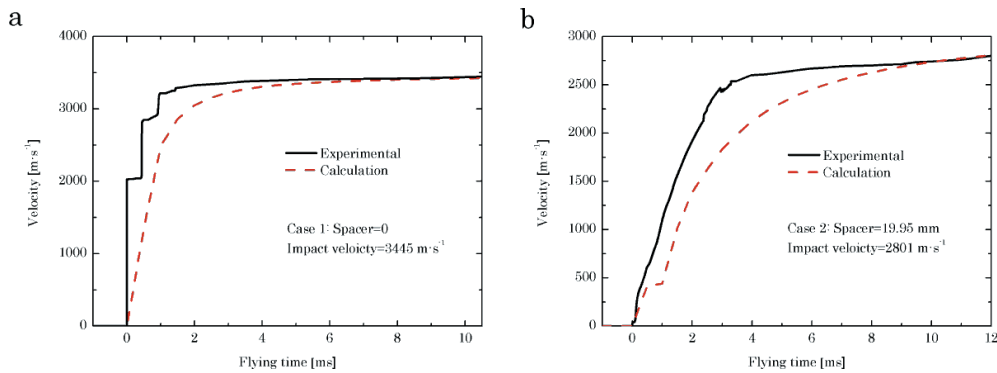


**Figure 2** Comparison of the velocity histories of impactor from the experimental data and numerical simulation.

classical theory of 1-D (one-dimensional) detonation<sup>20)</sup> or the numerical simulation of the impactor projection. Table 3 gives the results for the two impacting cases. The comparison of the velocity histories of impactor from the experimental data and numerical simulation is illustrated in Figure 2.

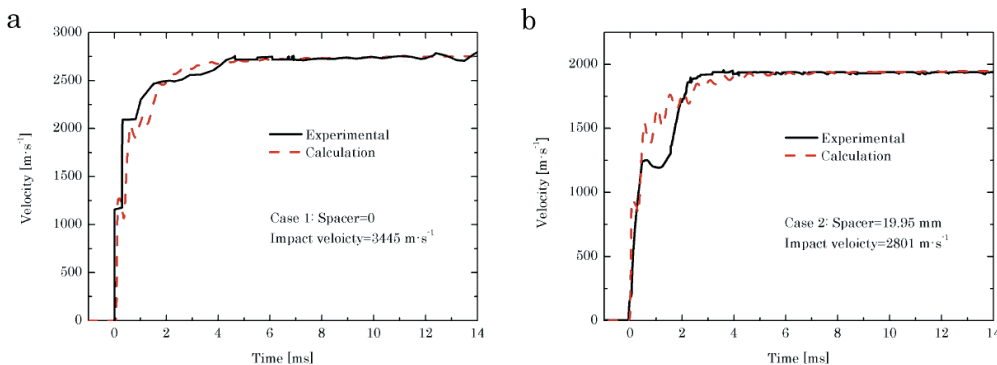
From the experimental data in Figure 2, we can find that the velocity histories rise to a plateau. For case 1 of the contact driving, the experimental velocity history undergoes a jump when the detonation wave loads to the impactor. Afterwards, the velocity profile sees several periodic growths due to the interreflection of shock and rarefaction wave in the impactor and affected by the thickness and density of the impactor, until it reaches the maximum horizontal value. However, the subsequent growth range is decreased. While for case 2 of non-contact driving, the rising edge of the velocity profile is not so steep as that in case 1 since the impactor is driven by the expansion of detonation products rather than the shock wave generated from detonation. Thus, the exist of the air spacer between the loading explosive and impactor makes the velocity acceleration process more smooth and maintains the original thermodynamic state and mechanical properties of the impactor, meanwhile makes the impact velocity lower. Nevertheless, the length of air spacer cannot be too long because a long spacer would

result to a strong lateral rarefaction wave which makes the movement of the impactor deviate from 1-D condition and affects the flatness of the impactor when it impacts with the sample explosive.

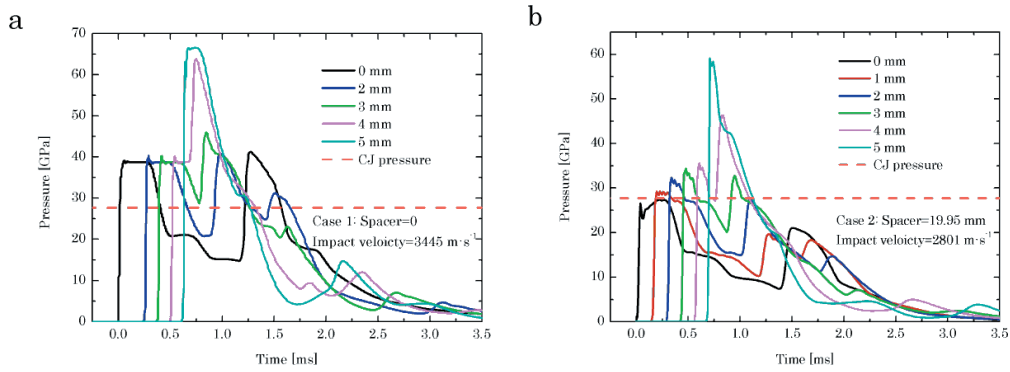
The impact velocity of the simulation results is very close to the experimental value (relative error is less than 2%), but the rising edge of the profile has a large difference. The main reason for this phenomenon is that the JWL EOS used for the detonation products cannot describe the expansion process of detonation products from high pressure to low pressure perfectly.

Figure 3 presents the velocity histories of flyer plate. For the experimental case 1, the velocity of the flyer soars to a small plateau of  $2000\text{ m}\cdot\text{s}^{-1}$  in  $1\ \mu\text{s}$ . While for case 2, the velocity of the flyer rises to a small plateau of  $1200\text{ m}\cdot\text{s}^{-1}$  in more than  $2\ \mu\text{s}$ . The higher impact velocity leads to a steeper rising edge and a higher final velocity plateau. In addition, the numerical results are in good correspondence with the experimental data-judged on the basis of waveforms and final velocity plateau.

Figure 4 overlays the calculated pressure histories at different locations in the TATB based explosive II. The distance labeled in the figure is the distance from the impacting surface to the gauge at the centerline of the cylindrical charge. As shown in Figure 4, the profiles give the ignition and increase trend of the pressure, and the



**Figure 3** Comparison of the velocity histories of flyer plate from the experimental data and numerical simulation.



**Figure 4** Calculated pressure histories at different locations in the sample explosive.

time interval between the impact moment and the time of arrival of detonation wave. In case 1, overdriven detonation occurs soon after the impact, and the peak pressure keeps steady around 40 GPa until the detonation wave is reflected from the aluminum flyer plate at the rear of the charge. While in case 2, a near CJ detonation pressure is acquired at the impact surface, later the peak pressure increases as the detonation wave propagates forward in the charge until it is reflected from the flyer. The peak pressure increases to a value higher than CJ pressure just 1 mm from the impact interface. This phenomenon is interesting, and should be experimentally measured and proved in the future.

## 5. Conclusion

In conclusion, an experimental and numerical study on the acceleration of flyer plate by overdriven detonation of insensitive high explosive is reported. The velocity histories of the flyer were measured by VISAR, and a numerical simulation of the whole system was conducted. The following conclusions can be drawn from current study:

- (1) Different impacting velocities lead to different detonation phenomena in the insensitive high explosive. Thus, different velocities of flyer plate are gained by different impacting velocities.
- (2) The numerical results of the flyer plate are in good correspondence with the experimental data by use of our modified model.
- (3) The modified model can simulate the overdriven detonation of insensitive high explosive in detail. A steady overdriven detonation and a CJ detonation to overdriven detonation transition are acquired respectively in our calculation.

## Acknowledgments

This research is funded by the National Natural Science Foundation of China (11372291, 11602238). We thank Dr. Shanggang Wen for his constructive suggestion on the final manuscript.

## References

- 1) W. Fickett and W. C. Davis, "Detonation", University of

- California Press (1979).
- 2) L. G. Green, C. M. Tarver, and D. J. Erskine, Proc. 9th Symposium (International) on Detonation, 195–202, Office of Naval Research, Arlington (1989).
- 3) J. N. Fritz, R. S. Hixson, M. S. Shaw, C. E. Morris, and R. G. McQueen, *J. Appl. Phys.*, 80, 6129–6141 (1996).
- 4) S. Maeda, S. Kanno, I. Yoshiki, and T. Obara, *Sci. Tech. Energetic Materials*, 77, 79–85 (2016).
- 5) A. B. Wenzel, *Int. J. Impact Eng.*, 5, 681–692 (1987).
- 6) J. Loiseau, J. Huneault, and A. J. Higgins, *Procedia Eng.*, 58, 77–87 (2013).
- 7) A. Geille, *Int. J. Impact Eng.*, 20, 271–279 (1997).
- 8) C. Sun, F. Zhao, S. Wen, Q. Li, and C. Liu, *AIP Conf. Proc.*, 429, 971–974 (1998).
- 9) Z. Liu, S. Kubota, and S. Itoh, *Int. J. Impact Eng.*, 26, 443–452 (2001).
- 10) E. L. Lee, H. C. Horning, and J. W. Kury, "Adiabatic expansion of high explosive detonation products", Lawrence Radiation Laboratory Report UCRL-50422 (1968).
- 11) Y. P. Lian, X. Zhang, X. Zhou, S. Ma, and Y. L. Zhao, *Int. J. Impact Eng.*, 38, 238–246 (2011).
- 12) C. A. Forest, Burning and detonation, Proc. 7th Symposium (International) on Detonation, 234–243, Office of Naval Research, Arlington (1981).
- 13) E. L. Lee and C. M. Tarver, *Phys. Fluids*, 23, 2362–2372 (1980).
- 14) J. N. Johnson, P. K. Tang, and C. A. Forest, *J. Appl. Phys.*, 57, 4323–4334 (1985).
- 15) K. Kim, Proc. 9th Symposium (International) on Detonation, 593–603, Office of Naval Research, Arlington (1989).
- 16) Z. Y. Zhang, F. Y. Lu, Z. B. Wang, and S. Huan, *Explos. Shock Waves* 19, 360–364 (1999). (in Chinese).
- 17) L. Green, E. Lee, A. Mitchell, and C. Tarver, Proc. 8th Symposium (International) on Detonation, 587–595, Office of Naval Research, Arlington (1985).
- 18) L. M. Barker and R.E. Hollenbach, *J. Appl. Phys.*, 43, 4669–4675 (1972).
- 19) G. McQueen, S. P. Marsh, J. W. Taylor, J. N. Fritz, and W. J. Carter, "The equation of state of solids from shock wave studies". In: *High-Velocity-Impact Phenomena* (ed. R. Kinslow), 293–417, Academic Press (1970).
- 20) C. Sun, Y. Wei, and Z. Zhou, "Applied detonation physics", National Defense Industry Press (2000). (in Chinese).